Carbon nanotube Josephson junctions

Henrik Ingerslev Jørgensen*†, Kasper Grove-Rasmussen*, and Poul Erik Lindelof

Nano-Science Center, Niels Bohr Institute, Denmark
These authors have contributed equally, †hij@fys.ku.dk

Abstract

We have succeeded in making reproducible superconducting contacts to gated single-walled carbon nanotubes (SWCNTs). Electrodes of two types of superconducting trilayers are fabricated; Ti/Al/Ti and Pd/Nb/Pd. We have devices ranging from the high transparency regime (Fabry-Perot (FP) regime) through the intermediate transparency regime (Kondo regime), to the low transparency regime (Coulomb blockade (CB) regime). In the CB regime, we report on a highly regular SWCNT quantum dot (QD). We analyze quasiparticle (QP) tunneling as function of gate voltage from resonance to off resonance (i.e. CB). In the FP regime we observe peaks in the differential conductance at $\pm 2\Delta/e$ due to the onset of quasi particle tunneling, and features at $\pm\Delta/e$ and $\pm 2\Delta/3e$ due to multiple Andreev reflections (MARs). We also observe a narrow peak in differential conductance around zero bias, which is interpreted as a noise smeared proximity induced supercurrent. This supercurrent and excess current are extracted at several different gate voltages and plotted as function of normal state conductance.

Keywords: Carbon nanotubes, Josephson junction, quantum dot, multiple Andreev reflections

1 Introduction

Electron transport through a SWCNT bridging two metal electrodes has been studied intensively over the last years. At low temperatures different transport regimes depending on the transparency of the metal-SWCNT interfaces have been identified. With low transparency contacts a quantum dot (QD) is defined in the SWCNT [1]–[4], and with intermediate transparency contacts Kondo resonances around zero bias are observed [5], [6]. High transparency contacts are in recent years also reported, where the SWCNT constitutes an electron waveguide with FP interferences [7], [8].

Changing the metal electrodes to superconductors dramatically change the transport characteristics. In such junctions where the SWCNT is making a weak link between two superconductors several interesting effects can be observed. At zero bias a supercurrent can flow through the weak link [9]–[11] due to the Josephson effect [12], while at low bias voltages current is determined by multiple Andreev reflections (MAR) [13]–[15] due to Andreev reflections (ARs) at the two SWCNT-S interfaces [16]. Furthermore, ARs give rise to an excess current.

In this article we present transport measurements on gated S-SWCNT-S Josephson junctions at low temperatures. The main points are the gate dependence of the QP current in a closed SWCNT QD, and the dependence of the excess current on normal state conductance in an open SWCNT QD.

2 Experimental

Two types of devices with different superconducting electrodes are made. For both types of devices we start by making a set of alignment marks by electron beam lithography (EBL) to align the additional layers. We first use the alignment marks to position islands of catalyst material. The SWCNTs are grown by chemical vapor deposition (CVD) from the catalyst islands in an oven at $\sim 900^o$C with a controlled flow of gasses; CH_4: 0.5 L/min, H_2: 0.1 L/min, and Ar: 1.1 L/min [17], [18]. After growth, source and drain electrodes consisting of superconducting trilayers are positioned next to the catalyst islands to contact the SWCNT. The gap between the source and drain trilayer films is approximately 500 nm.

For the first type of devices, we use a superconducting trilayer consisting of 5 nm titanium to make good contact to the SWCNT, then 40 nm aluminum to raise the transition temperature, and finally 5 nm titanium to stop oxidation of the aluminum. For the second type of devices, we use a trilayer of 5 nm Pd, 60 nm Nb, and 5 nm Pd, because Pd is known to make high transparency contacts to SWCNTs, and Nb has a high superconducting transition temperature T_C. However, in almost all of our devices we find that the Pd/Nb/Pd electrodes make poor contact to the SWCNT, with an average resistance around $\sim 100\,\mathrm{K}\Omega$ at room temperature.

The substrate, which we use as a backgate, is made of highly doped silicon with a 500 nm top layer of SiO_2.

A four probe device of the superconducting trilayers is defined to be able to measure the transition temperature

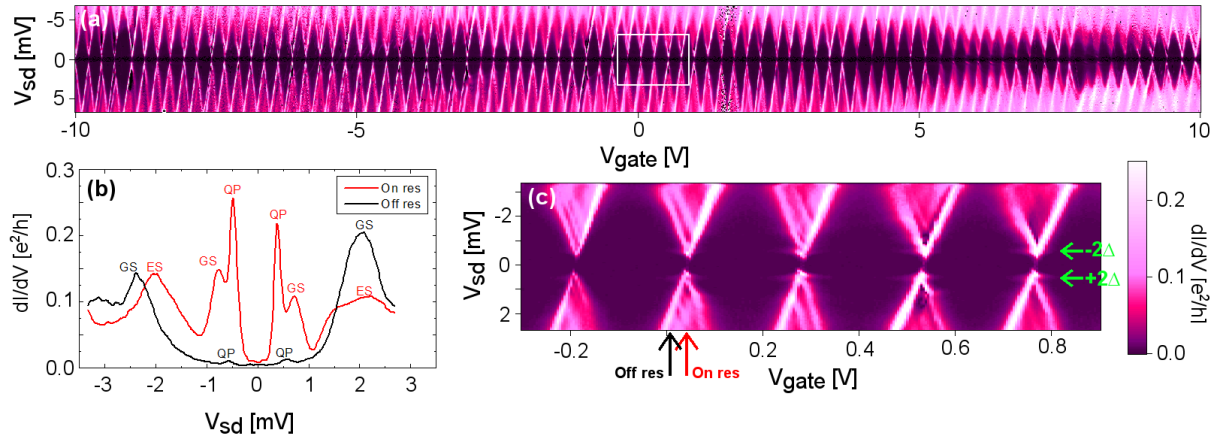

Figure 1: (a) dI/dV versus bias and gate voltage for a metallic SWCNT quantum dot with superconducting leads showing regular Coulomb blockade diamond structure. A narrow gap appears around zero bias due to superconductivity. (b) Bias cuts at gate voltages indicated in (c), where QP, GS and ES correspond to the onset of quasiparticle tunneling, tunneling through the ground state and excited state. (c) Zoom in of (a) showing the superconducting gap around zero bias (indicated with green arrows).

T_C and the critical field B_C at low temperatures. For the Ti/Al/Ti film, we find $T_C = 750\,\mathrm{mK}$, $B_C = 75\,\mathrm{mT}$ and from BCS theory a superconducting energy gap of $2\Delta = 3.5 k_B T_C = 230\,\mu e\mathrm{V}$ is calculated. As will be shown below this matches well with the sub gap structure (SGS) observed.

For the Pd/Nb/Pd film we find $T_C \sim 9\,\mathrm{K}$, which correspond to an energy gap of $\Delta \sim 1.5\,m e\mathrm{V}$. As will be shown below the onset of quasiparticle tunneling is at $V_{sd} \sim \pm 560\,\mu\mathrm{V}$ which corresponds to $\pm 2\Delta/e$. It therefore seems that the middle Nb layer of the Pd/Nb/Pd film has a high energy gap of $\sim 1.5\,m e\mathrm{V}$ but only a weak proximity effect on the Pd layer yielding an energy gap of $\Delta = 280 \mu e\mathrm{V}$.

All measurements are preformed at 300 mK in a sorption pumped ^{3}He cryostat (Oxford Instruments Heliox). The measurements are made with standard DAQ cards, lock-in amplifiers (excitation $5\mu V$), and opto-couplers to reduce noise.

3 SWCNT closed QD

Figure 1(a) shows a bias spectroscopy plot of a S-SWCNT-S QD measured at T=300 mK, below the critical temperature of the leads. Here the leads are made of Pd/Nb/Pd trilayers. The device shows a clear regular CB diamond structure with 83 electrons added to the QD in the gate range measured. No four period pattern is observed, but the regular pattern indicate a high quality metallic SWCNT. From the Coulomb diamonds an average charging energy of $U_C \sim 5.7\,m e\mathrm{V}$ and an average level spacing of $\Delta E \sim 1.3\,m e\mathrm{V}$ is deduced. The latter is estimated from the relative few excited states visible. Furthermore, a rough estimate of the line width Γ can be extracted from the current plateau of the ground state in the I-V curves assuming equal coupling, $\Gamma \sim 10 \mu e\mathrm{V}$. A gap in differential conductance is observed around zero bias, which is most pronounced in all of the resonances (charge degeneracy points). Such tunnel characteristic is consistent with the low transparency contacts between the SWCNT and the leads, because Andreev reflections are suppressed. In Fig. 1(c) this tunnel-like behavior is more clearly revealed in a zoom of a few Coulomb diamonds. The green arrows at $V_{sd} = \pm 560 \mu\mathrm{V}$ point to the horizontal lines attributed to the onset of QP tunneling reflecting the peaks in the density of states of the superconductors. The onset of quasiparticle tunneling is most visible when the level in the dot is resonant with the source and drain, but it is also visible in regions of CB. In the latter case quasiparticle tunneling happens via cotunneling processes.

Figure 1(b) shows cuts at two different gate voltages, in resonance (red) and slightly off resonance (black). The onset of quasiparticle tunneling is visible in both cases but suppressed off resonance due to CB and the sharpness of the level (Γ small). The peaks at higher bias voltages are due to tunneling through the ground state (GS) and the excited state (ES) of the QD. Slightly off resonance (black curve) no higher order Andreev reflection processes is visible for $|V_{sd}| < 2\Delta/e$ as expected due to suppression by CB. One Andreev reflection would be a fourth order process in the CB region and is thus highly suppressed. In resonance some structures are visible at low bias, which could be due to higher order Andreev reflection. In fact all the even order (n) Andreev pro-

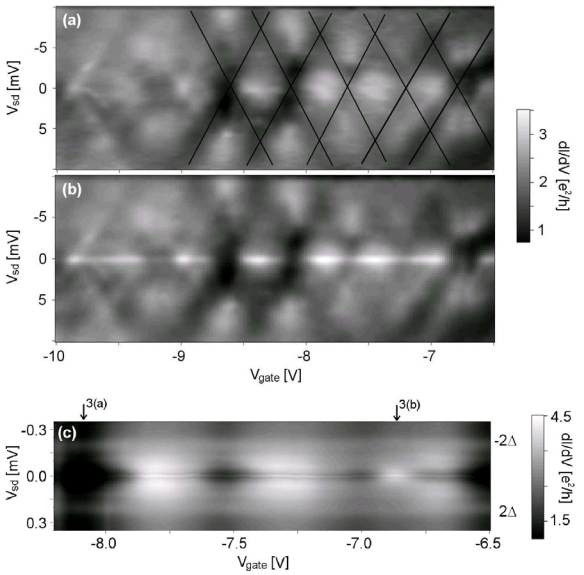

Figure 2: (a) shows a bias spectroscopy plot in the high transparency gate region, with a small magnetic field (B=100 mT) to suppress the superconducting state of the electrodes. (b) is analog to (a) but without magnetic field, i.e. with superconducting electrodes. In (c) we show a zoom-in around small source drain voltages where the excess current is observed. Arrows are pointing to the gate voltages where the graphs in Fig. 3(a-b) are measured.

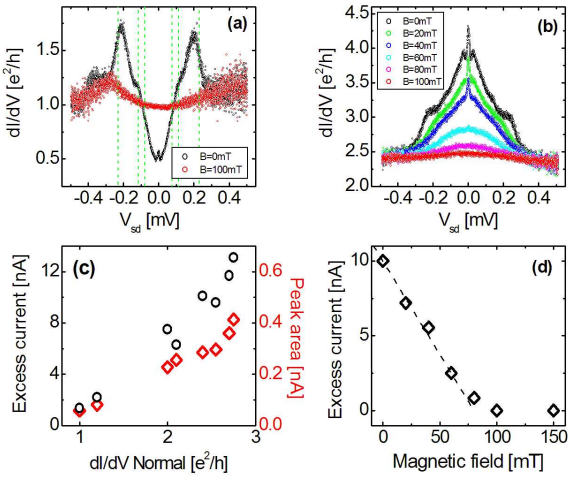

Figure 3: (a) and (b) is differential conductance versus source drain voltage measured with lock-in amplifier (5 μV excitation) at different gate voltages as indicated in Fig. 2(c). Black is with superconducting electrodes and red is with 100 mT magnetic field to suppress the superconductivity of the electrodes. (a) is measured at an antiresonances of the Fabry-Perot pattern and (b) is measured at a resonance with increasing magnetic fields applied. (c) Excess current and peak area (supercurrent) is extracted as described in the text and plotted as function of normal state conduction. (d) Excess current versus magnetic field, extracted from (b).

cesses should be suppressed at resonance [19]–[21], [14], while the odd is enhanced. At resonance small features appear at $V_{sd} \sim \pm 100 \mu e$V which might stem from the n = 3 (2 ARs) process. It is also seen that the lines stemming from QP tunneling seems to be positioned at slightly lower bias on resonance than off resonance, which is qualitative consistent with theory describing transport through a resonant level.
Even though a supercurrent through a quantum dot has been predicted theoretically [22], we observe no sign of it in these measurements.

4 SWCNT open QD

The second device is made with the Ti/Al/Ti superconducting trilayer. For this film we typically observe much higher transparency than with the Pd/Nb/Pd film. The reported device is in the FP regime, i.e. the SWCNT defines an open QD. Compared to the device above, we no longer have single electron transport. Electrons are now continuously added to the QD, and the oscillations in conductance seen in the bias spectrum in Fig. 2 reflect the discrete energy spectrum of the QD.
Figure 2(a) shows a bias spectroscopy with a small magnetic field applied ($B = 100mT$) to suppress the superconducting state of the electrodes.
The average differential conductance in this gate region is around $\sim 2.5e^2/h$ with maximums of about $\sim 3e^2/h$, approaching the theoretical limit of $4e^2/h = (6.5k\Omega)^{-1}$. As V_{gate} and V_{sd} are changed the dips in conductance evolve into straight lines, forming a mesh of crossing dark lines. These pronounced oscillations in differential conductance versus V_{gate} and V_{sd} are clear signs of the FP interference [7].
As we turn off the magnetic field, i.e. turn on the superconducting state of the electrodes, an overall increase in differential conductance between $V_{sd} \sim \pm 2\Delta/e$ is observed (Fig. 2(b)). A more detailed bias spectroscopy plot of this overall increase through three resonances is shown in Fig. 2(c). As will be described in more detail below this increase includes a rich sub gap structure.
Detailed measurements with lock-in amplifier of differential conductance versus V_{sd} at gate voltages indicated in Fig. 2(c) are shown in Fig. 3(a-b), where (a) is through an antiresonances and (b) is through a resonance.
A characteristic conductance variation between $V_{sd} \sim \pm 2\Delta/e$ is seen for all gate voltages. The change in conductance between $V_{sd} \sim \pm 2\Delta/e$ to typically higher, but also lower values than the normal state differential conduction G_N, is because superconductivity induced

transport mechanisms occur.

A general trend in our S-SWCNT-S junctions with high transparency is a sub gap structure (SGS) [23]–[28] with features at $|V_{sd}| = 2\Delta/en$ for $n = 1, 2, 3$, and a peak around zero bias. The peak around zero bias has a full width of only $\sim 25\mu V$, and persists at all gate voltages in the FP-region. This zero bias peak might be due to a noise smeared proximity induced supercurrent. A supercurrent is normally seen as a dissipationless current. However, for a small supercurrent where the Josephson energy $E_C = \hbar I_C/2e$ is smaller then the temperature, phase fluctuations will smear the supercurrent into a conductance peak [12]. To characterize this possible supercurrent we therefore estimate its magnitude in accordance with the resistive shunted junction (RSJ) model as the area of the peak (not the whole area under the peak since the voltage dependent resistor in the RSJ model includes all normal current as well as current due to the MARs at finite biases). The maximum supercurrent estimated in this manner is around $\sim 0.5\,\mathrm{nA}$, which corresponds to a Josephson energy of only $\sim 10\,\mathrm{mK}$. This is much smaller than the temperature of the cryostat (300 mK). We have in another device with lower transparency observed a dramatic increase of the peak area as function of temperature below 100 mK [18]. A similar behavior could therefore be expected for the here reported device.

For several of our high transparency S-SWCNT-S junctions we have observed an excess current that depends on G_N. Excess current is defined as the difference in current between having the electrodes in the superconducting state and the normal state at $V_{sd} \gg \Delta/e$. It is therefore found as half of the difference in area between the black and red curves in Fig. 3(a-b).

In Fig. 3(c) we have extracted the excess currents and zero bias peak area (supercurrent) at 8 different gate voltages and plotted them as function of normal state conduction. The excess current scales with normal state conductance, and seems to have a small increasing slope towards higher normal conduction. The peak area has about the same dependence, but it is about 30 times smaller.

In Fig. 3(d) the excess current is plotted as function of applied magnetic field (extracted from Fig. 3(b)). The excess current falls off linearly with magnetic field, with zero excess current close to the critical field of the film (75mT).

5 Conclusion

In conclusion we have successfully fabricated gated S-SWCNT-S Josephson junctions with low transparency as well as high transparency contacts. In the Coulomb blockade regime we observe gate dependent onset of quasiparticle tunneling. In the Fabry-Perot regime we observe quasiparticle tunneling at $|V_{sd}| = 2\Delta/e$, features of MARs at $|V_{sd}| = 2\Delta/en$ for $n = 2, 3$, and a conductance peak around zero bias, which is interpret as a noise smeared proximity induced supercurrent. This supercurrent and excess current scales linearly with the normal conductance of the junction.

acknowledgments

We wish to acknowledge the support of the Danish Technical Research Council (The Nanomagnetism framework program), EU-STREP Ultra-1D program and the Nano-Science Center, University of Copenhagen, Denmark.

REFERENCES

[1] S. Tans et. al., Nature **386**, 474 (1997).
[2] M. Bockrath et. al., Science **275**, 1922 (1997).
[3] D. H. Cobden and J. Nygård, Phys. Rev. Lett. **89**, 046803 (2002).
[4] P. J. Herrero et. al., Nature **429**, 389 (2004).
[5] J. Nygård, D. H. Cobden and P. E. Lindelof, Nature **408**, 342 (2002).
[6] B. Babic et. al., Phys. Rev. B **70**, 235419 (2004).
[7] W. Liang et. al., Nature **411**, 665 (2001).
[8] J. Cao et. al., Phys. Rev. Lett. **93**, 216803 (2004).
[9] P. J. Herrero et. al., Nature **439**, 953 (2006).
[10] J. Haruyama et. al., Phys. Rev. B **68**, 165402 (2003).
[11] A. Y. Kasumov et. al., Science **284**, 1508 (1999).
[12] M. Tinkham, "Introduction to superconductivity", McGraw-Hill, 201 (1996)
[13] A. F. Morpurgo et. al., Science **286**, 263 (1999).
[14] M. R. Buitelaar et. al., Phys. Rev. Lett. **91**, 057005 (2003).
[15] M. R. Buitelaar et. al., Phys. Rev. Lett. **89**, 256801 (2002).
[16] A. F. Andreev, Zh. Eksp. Theor. Fiz. **46**, 1823 (1964).
[17] J. Kong et. al., Nature **395**, 878 (1998).
[18] K. Grove-Rasmussen, H. I. Jørgensen and P. E. Lindelof, cond-mat/0601371 (2006).
[19] A. L. Yeyati et. al., Phys. Rev. B **55**, 6137 (1997)
[20] G. Johansson et. al., Phys. Rev. B **60**, 1382 (1999)
[21] G. Johansson et. al., Physica C **293**, 77 (1997)
[22] L. I. Glazman et. al., J. Exp. Theo. Phys. Lett. **49**, 659 (1989).
[23] G. E. Blonder et. al., Phys Rev. B **25**, 4515 (1982).
[24] T. M. Klapwijk et al., Physica B+C **109-110**, 1657 (1982).
[25] P. E. Gregers-Hansen et. al., Phys Rev. Lett. **31**, 524 (1973).
[26] M. Octavio et. al., Phys Rev. B **27**, 6739 (1983).
[27] J. C. Cuevas et. al., Phys. Rev. B **70**, 214512 (2004)
[28] A. Martin-Rodero et. al., Superlattices and Microstructures **25**, 925 (1999).